Available online at www.sciencedirect.com
SCIENCE DIRECT
Journal of Power Sources 156 (2006) 533–540
JOURNAL OF POWER SOURCES
www.elsevier.com/locate/jpowsour

Redox behavior of nanohybrid material with defined morphology: Vanadium oxide nanotubes intercalated with polyaniline

Marcos Malta [a], Guy Louarn [b], Nicolas Errien [b], Roberto M. Torresi [c,*]

[a] *Instituto de Química de São Carlos, Universidade de São Paulo, CP 780, 13560-970 São Carlos (SP), Brazil*
[b] *Institut des Matériaux Jean Rouxel, Université de Nantes, BP 32229, 44322 Nantes, France*
[c] *Instituto de Química, Universidade de São Paulo, CP 26077, 05513-970 São Paulo (SP), Brazil*

Received 4 May 2005; accepted 16 May 2005
Available online 14 July 2005

Abstract

Vanadium oxide/polyaniline nanotubes were produced by cationic exchange between hexadecylamine and polyaniline after the synthesis of vanadium oxide nanotubes by sol–gel method followed by hydrothermal treatment. The local structure of this hybrid material was studied by high-resolution transmission electron microscopy, infrared and Raman spectroscopy and small angle X-ray diffraction technique. The results show that polyaniline is intercalated in the interlamellar space of the vanadium oxide nanotube forming a hybrid material with defined morphology. Electrochemical impedance spectroscopy experiments have shown that the apparent diffusion coefficient for nanotubes with template was approximately 1×10^{-9} cm^2 s^{-1}. Nanotubes with polyaniline presented an apparent diffusion coefficient at least one order in magnitude higher than the parent material "with template", comparable with other vanadium oxide described in the literature, revealing a promising material for utilization as cathode for ion-Li batteries.

Keywords: Nanostructures; Polyaniline; Vanadium oxide; Nanocomposites; Lithium intercalation

1. Introduction

One of the most important aspects of the matter is concerned with its structure. Well-defined morphologies in the nanometric world such as nanotubes, nanofibers and spherical nanoparticles generally mean new physical and/or chemical properties for known compounds. Classical examples are carbon nanotubes: despite graphite is the most stable carbon compound, its properties (like the conductivity and magnetism) change drastically in the nanotubular shape. The ability to form nanotubes seems to be an inherent characteristic of 2D-layered materials. Tenne [1] has stated that lamellar nanoparticles are extremely reactive in the prismatic plane and one way to sature the dangling bonds in the periphery (edges) is by means the formation of nanotubes and fullerenes structures. As well as pioneer carbon [2], nanotubes based on metallic chalcogenides and oxides, have been synthesized by several groups in the world [3–5].

Another interesting subject related to nanostructures is the synergism. In general, this phenomenon could be described as the combination of positive features of two or more compounds, to generate a new material (called composite) with improved properties compared with the original components separately [6]. A special case of synergism occurs when the components are transition metal oxides and conducting polymers which, interacting at molecular level (by different type of chemical links, as hydrogen bonds, or short distance strength), form an exceptional class of electroactive nanocomposites. Among several examples, vanadium oxide is one of most studied material to be applied as inorganic matrix in nanocomposites. This compound has a structural versatility, which allows intercalating a wide variety of inorganic (and organic) guest species. For instance, the oxidative polymerization of aniline in the

* Corresponding author. Tel.: +55 11 30912350; fax: +55 11 38155579.
E-mail address: rtorresi@iq.usp.br (R.M. Torresi).

0378-7753/$ – see front matter © 2005 Elsevier B.V. All rights reserved.
doi:10.1016/j.jpowsour.2005.05.044

intralamellar space produces a nanohybrid material with higher electronic and ionic conductivity [7–10].

Early works made by Nesper et al. [11–13] demonstrated the viability of producing hybrid vanadium oxide/surfactant nanotubes (NT-VO_x), obtained by intercalation of alkylamonium ions in the lamellar vanadium oxide array, followed by hydrothermal treatment. These nanotubes are easily obtained as the main product starting from crystalline V_2O_5 [14], xerogel V_2O_5 [15], $VOCl_3$, NH_4VO_3, [16] $VO(OPr_2)_3$ [17] and aliphatic amines, which act as template. Unfortunately, the template surfactant molecules probably participate in redox reactions of NT-VO_x, diminishing the electroactivity of the material [17]. However, due to the structural flexibility of oxide network, template molecules can be partially substituted by metallic cations as Na^+, Ca^{2+}, K^+, Mn^{2+} or Cu^{2+} via an exchange reaction preserving the nanotubular shape and improving the electrochemical performance [18–20].

We believe that the insertion of conducting polymers in NT-VO_x would open new research fields to new applications for this anisotropic structure due to synergistic effect between these two species. It is well known that polyaniline (Pani) can be solubilized in several common organic solvents in the conducting form. The doping process by organic acid as camphorsulfonic or dodecylbenzenesulfonic acid provides the charge compensation beyond solubilizing the polymeric chain in *m*-cresol, chloroform, toluene and dimethylsulfoxide solvents [21,22]. In this article results about a new structured nanocomposite constituted by anisotropic vanadium oxide/Pani nanotubes (NT-VO_x/$Pani_y$), are presented. Starting from NT-VO_x/hexadecylamine as precursor, oxide nanotubes with Pani intercalated in the intralamellar space were obtained by cationic exchange reaction. The synthesis of an electroactive oxide as vanadium oxide with a defined morphology with a conducting polymer as Pani intercalated, can be important for electrointercalation process where solid diffusion and electronic conductivity are the main limiting factors for the charge transfer rate; so that, controlling morphology at the nanometric level it would be possible to reduce the diffusion length and increase electronic conductivity with the polymer.

2. Experimental

Vanadium oxide nanotubes were synthesized following the method developed by Nesper and co-workers [11]. For a typical synthesis procedure, 3.09 g of crystalline V_2O_5 (Merck) was slowly added in a beaker containing a transparent ethanolic solution (5.7 mL) of hexadecylamine 90% (4.55 g, Aldrich). The mixture was maintained under vigorous stirring during two hours and, after that, 16.7 mL of purified water (Milli-Q–Millipore system) was added. This material was aged during 48 h. Finally, a hydrothermal reaction was carried out in a "home-made" autoclave apparatus (capacity 50 mL) at 180 °C during 7 days. In order to remove the excess of hexadecylamine molecules, the final product was washed with water and absolute ethanol and dried under vacuum.

Pani was produced via chemical synthesis. An acid solution of ammonium persulfate (1.0 mol L^{-1} camphorsulfonic acid (HCSA) and 0.1 mol L^{-1} ammonium persulfate) (100 mL) was slowly added to 100 mL of aniline acid solution (1.0 mol L^{-1} HCSA and 0.1 mol L^{-1} aniline). The reaction was processed during 1.5 h at 25 °C due to relatively slow polymerization kinetics of aniline when the dopant is HCSA. After that, the polymer was filtrated and carefully rinsed with an aqueous solution of HCSA 1.0 mol L^{-1} and dried at approximately 100 °C during 2 days.

To obtain the hybrid V_2O_5/Pani nanotubes, cationic exchange reaction was performed in order to substitute protonated hexadecylamine molecules by Pani. For this purpose, 270 mg of vanadium oxide/hexadecylamine nanotubes were added to a Pani solution (approximately 350 mg Pani/CSA solubilized in 50 mL of chloroform). The sample was maintained under magnetic stirring during 10 h and after this period, the material was filtered, rinsed with absolute ethanol and dried at 90 °C. The partial substitution of hexadecylamine by Na^+ was done by stirring 260 mg of nanotubes suspension in a hydroalcoholic solution (40 mL of H_2O + 160 mL CH_3CH_2OH) of NaCl (260 mg) during 10 h at 25 °C.

FT-IR analysis (ATR mode) was performed in a Nicolet 20SCX FT-IR spectrometer. Raman spectra were recorded on a Renishaw Raman imaging microscope (system 3000) with an Olympus metallurgical microscope and a CCD detector. The samples were excited with the 632.8 nm line of a He–Ne laser (Spectra Physics, model 127). Laser power was always kept below 0.7 mW at the sample, in order to avoid thermal degradation.

X-ray powder diffraction was obtained in a Siemens D5000 powder diffractometer using Cu Kα radiation ($\lambda = 1.5406$ Å). Scanning electron microscopy analysis (SEM) have been run in a JEOL JSM-59000LV microscope and transmission electron microscopy (TEM) experiments have been performed with the JEM-3010 ARP microscope operated at 300 kV, both of the LME/LNLS, Campinas, Brazil.

For the electrochemical experiments, a conventional three electrodes cell was used with Li metal as reference and counter electrodes and a 1.0 mol L^{-1} solution of $LiClO_4$ in propylene carbonate as the electrolyte. The working electrode was prepared by 'painting' on a grid of steel the mixture constituted by electroactive material (80% in weight), electronic conductor (Vulcan® carbon 15%) and polyvinylidene fluoride (5%). Cyclic voltammetry (CV) and electrochemical impedance spectroscopy (EIS) experiments were carried out in an argon atmosphere using a potentiostat/galvanostat AUTOLAB model PGSTAT 30 from Ecochemie. During the EIS experiments, a potential modulation (5 mV rms) was imposed varying the frequency between 10 and 1.5 mHz.

3. Results and discussion

VO_x-NT can be characterized as a "lamellar rolling up structure" separated by surfactant molecules. Depending of the chain length of the template, the distances between the oxide layers can vary from 16.6 Å for butylamine to 38 Å, when docosylamine is used [23]. Recently, it was proposed that the basic element of NT-VO_x wall structure is V_7O_{16}, which comprises two sheets of VO_5 square pyramids with VO_4 tetrahedrals connecting these sheets [23]. The synthesis of this material occurs in two steps: in the first one, the intercalation of alkylammonium ions in the lamellar precursor provokes a diminution of the van der Waals strengths between the layers; the second step is the hydrothermic treatment, where enough energy is supplied to the system provoking the rolling up process of layers (in order to maintain a minimum contact) producing VO_x/alkylammonium-NT. The images obtained by SEM technique (Fig. 1a) show that practically all the final product presents a tubular morphology. It can be also noted that the major part of the tubes has an open extremity as can be verified through image obtained by TEM of an isolated Na_yVO_x-NT (Fig. 1b). This fact is very important regarding electrochemical insertion of Li^+ because the accessibility of internal channels by electrolyte can provide a rapid transport of ions to insertion sites. We will come back to this point later. Typical dimensions of nanotubes are in agreement with other data in literature [11–13], the tubes

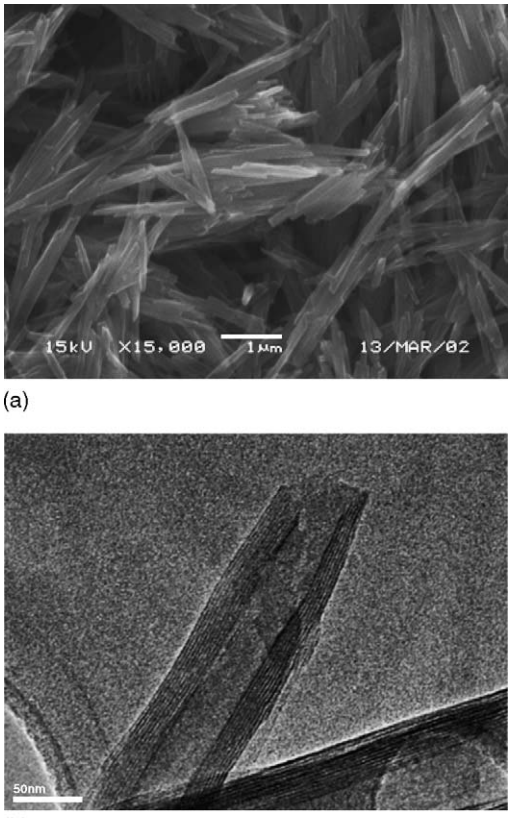

Fig. 1. (a) SEM and (b) HRTEM images of Na_yVO_x-NTs.

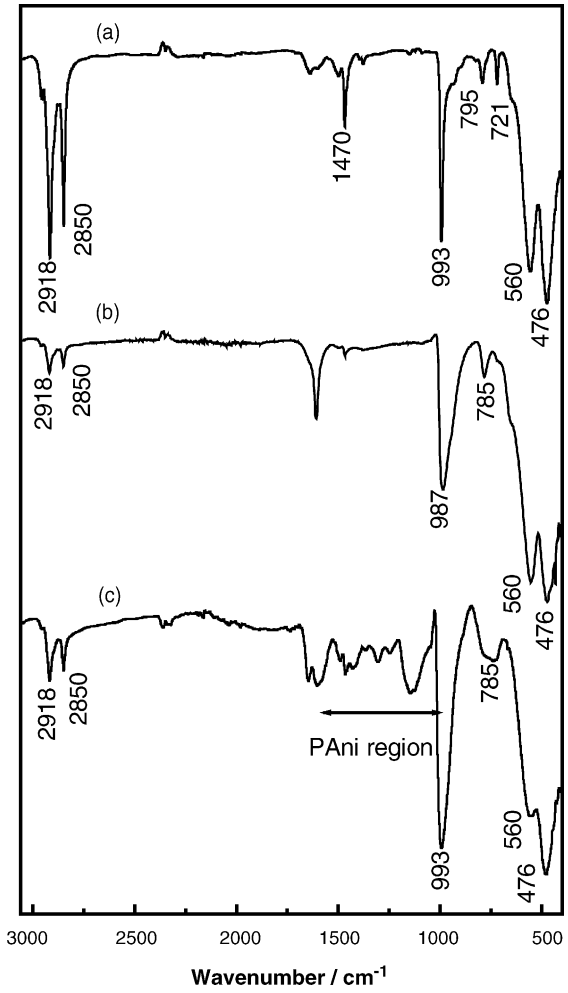

Fig. 2. FT-IR spectra of nanotubes of (a) VO_x/hexadecylamine, (b) Na_yVO_x and (c) $Pani_yVO_x$.

presenting a variable length from 1 to 10 μm while external diameters vary from 15 to 150 nm and internal diameters vary from 5 to 50 nm.

FT-IR measurements were carried out in order to characterize the materials individually and to verify the extension of both Na^+ and Pani exchange in the VO_x-NT. After hydrothermal treatment, crystalline V_2O_5 and hexadecylamine-intercalated templates are converted in the nanocomposite VO_x/hexadecylamine-NT (with template in the protonated form). Fig. 2a shows the FT-IR spectrum for VO_x/hexadecylamine-NT and it is possible to observe the four characteristic bands of the vanadium oxide at 993, 795 and 550–450 cm^{-1} corresponding to V=O, V–O–V asymmetric stretch, and V–O–V symmetric stretch mixed with the deforming vibrations of the vanadium oxygen polyhedra, respectively [24]. Hexadecylamine molecules present bands at 2918 and 2850 cm^{-1} related to the axial stretching of aliphatic C–H, at 1469 cm^{-1} related to symmetric angular deformation in the plane of CH_2 species and at 721 cm^{-1} resulting from the symmetric out of plane angular deformation of N–H species.

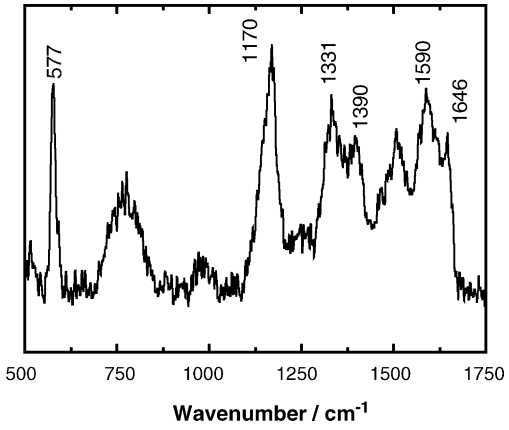

Fig. 3. Raman spectrum of nanotubes of $Pani_yVO_x$.

Spectra in Fig. 2b correspond to the material obtained after exchange reaction with metallic cations; that is to say, when most part of protonated hexadecylamine molecules was substituted by Na^+ ions. It can be visualized a decrease in the relative intensity of the bands corresponding to the template indicating a partial substitution of surfactant molecules. In this spectrum it is also possible to note a small shift of vanadyl band (V=O) to lower frequencies in relation to the material with template. This same behavior is observed when FT-IR spectra of vanadium oxide intercalated with different species are compared; this phenomenon is basically due to the different chemical interactions between ions (and molecules) and the host structure. For example, Nazar and co-workers [25] verified that asymmetric and symmetric stretchings for the V_2O_5/polypyrrole nanocomposite shift to higher wave numbers with the increase of polymer content. Also, the band related to V=O stretching shifts to lower wave numbers due to the contribution of hydrogen bonds between the polymer and the oxide. This shifting to lower wave numbers of the vanadyl band is also observed during the intercalation of Li^+ in V_2O_5 films due to interactions V=O–Li^+ and the presence of V^{4+}/V^{5+} sites.

VO_x/$Pani_y$ FT-IR spectra (Fig. 2c) can be divided in two main regions: below 1010 cm^{-1} corresponding to the oxide component, and from 1050 to 1800 cm^{-1} corresponding to the polymeric part. The intensity of the surfactant doublet at higher wave numbers also decreases indicating a partial hexadecylamine substitution by Pani. In other words, FT-IR spectroscopy is a useful tool to verify that, at least in some extend, the polymer interacts with the inorganic matrix.

In order to analyze in more details the oxidation state of Pani in the material, Raman spectroscopy [26] was employed due to the fact that, because of resonant effect, the spectrum of the polymeric material is enhanced (Fig. 3). The spectrum is consistent with previously reported spectra for Pani [26]. Specifically, the bands at 1170, 1331 and 1590 cm^{-1} are characteristic of benzenoid segments, polaronic structures, and quinoid segments, respectively. It is clear in the spectrum that Pani is in the "emeraldine like form" due to the high intensity of the 1331 cm^{-1} band, related to the C–$N^{\bullet+}$ stretching. The three bands located at ca. 577, 1390, and 1646 cm^{-1} should be also noted. These bands are related to cross-linked segments [26] leading to the formation of other structures than radical ones, such as ternary cyclized nitrogen producing "phenazine-like" segments. Rodriguez et al. [27] have shown from XPS experiments that thermally treated protonated forms of polyaniline, originate cyclized nitrogen species specially in detriment of imine segments, with this cyclization reaching a maximum in the case of sulfonate-doped polyanilines.

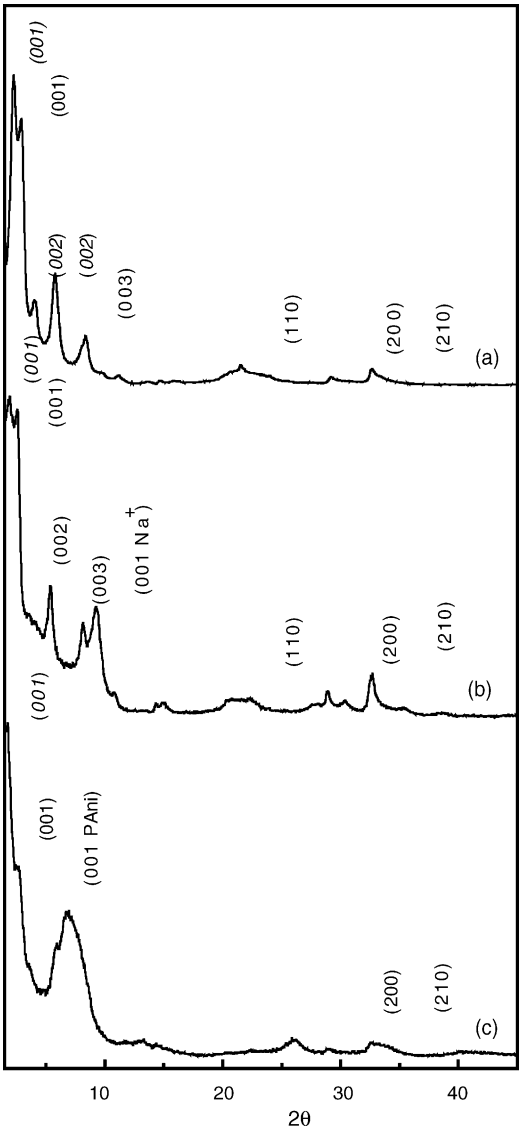

Fig. 4. XRD spectra of nanotubes of (a) VO_x/hexadecylamine, (b) Na_yVO_x and (c) $Pani_yVO_x$.

X-rays diffraction (XRD) experiments (Fig. 4a) were carried out in order to evaluate the basal distance in the nanotubes by (0 0 *l*) reflections and in this form to verify if the polymer is intercalated in the interlamellar space. The NT-VO_x/hexadecylamine presented two kinds of intralamellar

distances, where the first peak with the highest intensity corresponds to a d value of 44.3 Å (1.98°, d_{001}) and the second one reflects the distance of 33.8 Å (2.61°, d_{001}). This fact was also found in the case of nanotubes synthesized from NH_4VO_3 and octadecylamine or 1,6-hexamethrlenediamine [16], and it was explained by the difference in the overlap of the alkyl chains or/and different tilt angles. Fig. 4b shows the XDR pattern for nanotubes after cationic exchange reaction with Na^+. It is observed a new peak at 9.24° corresponding to a basal distance of 9.6 Å. Since substitution of hexadecylamine by Na^+ is not complete, the other peaks related with the alkyl chains are also observed. When the cationic exchange reaction was done with Pani (Fig. 4c), it is observed a double peak at 5.95 and 6.95° corresponding to basal distances of 14.8 and 12.9 Å, respectively. These two values are close to data reported in the literature [7,8] when one monolayer of Pani is inserted in vanadium oxide xerogel. The small shoulder observed at 2.62° (33.7 Å) indicates that a certain amount of surfactant still remains deeply inserted in the nanotubes. This XRD pattern clearly shows that Pani substitutes the alkyl chain, in this way forming an electroactive hybrid material. Reflections localized at higher angles ($2\theta > 15°$), are originated from a bi-dimensional structure of the layers of vanadium oxide. These peaks are independent on the intercalating species and indicate that cationic exchange reaction do not cause changes in the oxide layer.

After exchange reaction the structure and morphology of the samples were examined by high-resolution transmission electron microscopy (HRTEM). Fig. 5a shows a micrograph at low magnification where the tubes appear in both isolated and bundles forms. Some amount of Pani could be deposited on the surface of the nanotubes and would be responsible by anisotropic charge distributions over all part of the nanostructure. Moreover, it must not be ignored the hypothesis that some amount of Pani/CSA remains without reacting with the oxide. Fig. 5b shows the tubes as a layered structure with open ends and an external diameter of typically 70 nm, but it was observed a diameter range from 25 to 80 nm. The tube length obtained varied from 1 to 10 μm. The layered structure of the walls appears as alternating fringes of dark and bright contrast, where in agreement with the structure proposed for vanadium nanotubes [11–13], dark fringes correspond to vanadium oxide layers. Between these layers the conducting polymer is intercalated as it was shown by XRD experiments. In order to observe in more detail the layered structure of nanotubes walls, a higher magnification was used, as it is shown in Fig. 5c. The distance between vanadium oxide layers calculated from the small angle values of the (0 0 l) reflection of XRD patterns are similar to that obtained by HRTEM images, being typically 1.4 nm. These figures also demonstrate that the substitution of hexadedylamine by Pani does not affect the morphology of the vanadium oxide nanostructure.

The exchange cationic reactions in NT-VO_x can only occur if the ratio V^{4+}/V^{5+} is maintained because, as it was shown, the tubular shape is conserved. Probably, the driving force for the exchange reaction is the solubility of alkyl chain

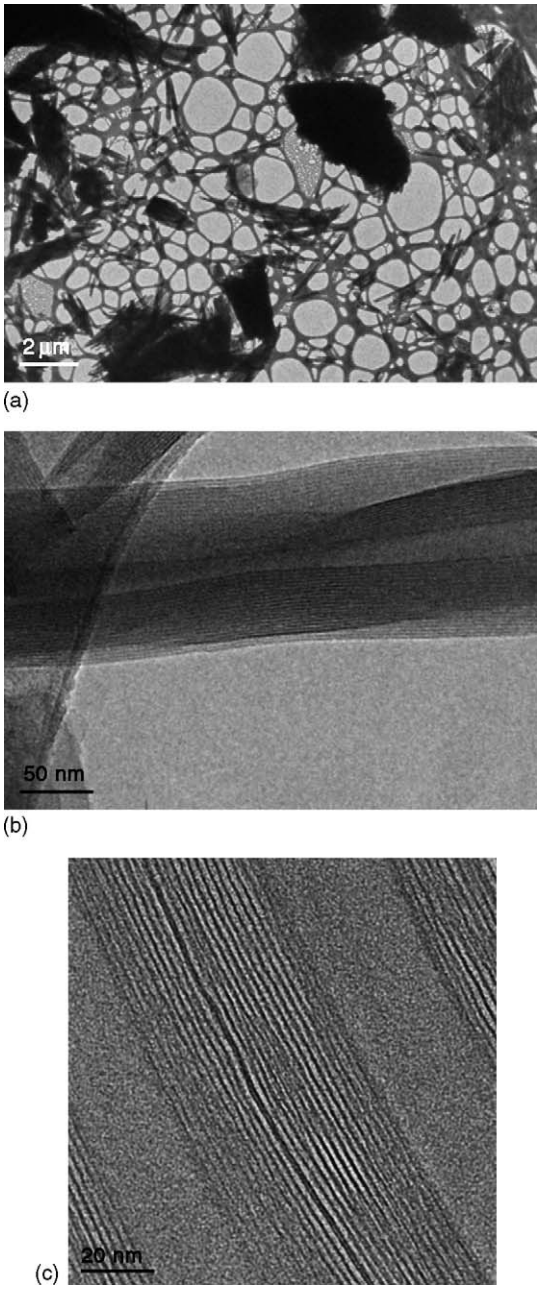

Fig. 5. TEM micrographs at different magnifications of the hybrid nanotubes with Pani: (a) bundle of nanotubes, (b) isolated one and (c) high magnification of the layered walls.

in organic solvents, coupled with the concentration gradient generated due to the relative small amount of surfactant (inside of nanotubes) related to positive species in the reaction environment. Obviously, the mechanism proposed for the exchange reaction of hexadecylamine by Pani is based in the principle of electroneutrality: the intercalation process of Pani in the nanotubes (where the negatively charged oxide network counter-balances the semi-oxidized Pani) is concomitant with the expulsion of protonated hexadecylamine.

With the objective of evaluating the electrochemical performance of VO_x/$Pani_y$-NT as cathodic material, electro-

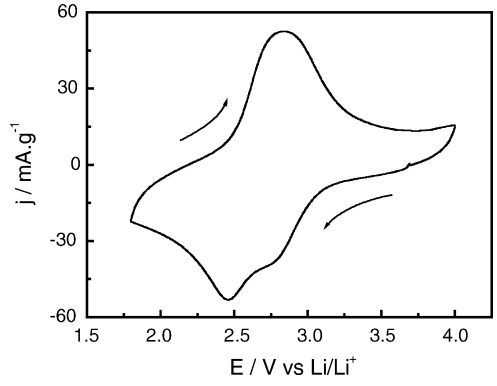

Fig. 6. Cyclic voltammetry of VO_x/$Pani_y$-NT. Scan rate: 50 μV s^{-1}. Electrolytic solution: 1.0 mol L^{-1} $LiClO_4$ in propylene carbonate.

chemical experiments as CV and EIS were carried out. The CV experiment (Fig. 6) started from open circuit potential (3.60 V versus Li/Li^+), scanning in the negative going direction until 1.8 V and then, scanning in the positive going direction until 4.0 V. Two cathodic current peaks at 2.75 and 2.45 V are observed corresponding to lithium intercalation in the nanotubes as a consequence of vanadium reduction. In the oxidation process, just a broad peak localized at 3.8 V is observed and corresponds to the deintercalation of Li^+. It must be notice that, as a consequence of synergistic effect between the two components, the nanocomposite with tubular shape is electroactive in this range of potential.

EIS experiments for nanotubes were made in order to verify how the morphology and the different guest species (Pani, hexadecylamine and Na^+) affect the electrochemical response of this material. Three samples were selected: VO_x/hexadecylamine-NT, Na_yVO_x-NT and VO_x/$Pani_y$-NT. In an ideal behavior, extrapolating the semi-circle to low frequencies region of a Nyquist diagram, it is possible to calculate the electronic resistance of the material. But, as can be observed in Fig. 7 (a–c), the electronic transport occur with a time constant near to the diffusional process, and we can not determine with precision the resistance of the electrodes. However, just analyzing Fig. 7 we can say that resistance of VO_x/hexadecylamine-NT electrode is higher than those of the other ones. In fact, we can expect that the electronic resistance would be smaller after exchange reaction with Na^+ and Pani in the nanotubes. This small resistance in the nanocomposite nanotubes would be a consequence of the intercalation of electroactive Pani in the interlamellar space. It is well known that the electronic conductivity is an anisotropic property of lamellar materials, interlamellar conductivity being smaller than intralamellar one. The presence of Pani would decrease the ohmic drop and provide an alternative conducting way in order to interconnect the isolated nanotubes, which become electrochemically active. In contrast with this fact, VO_x/hexadecylamine-NT electrodes are more resistive because the isolating character of template molecules can decrease the interlayer electronic mobility (in

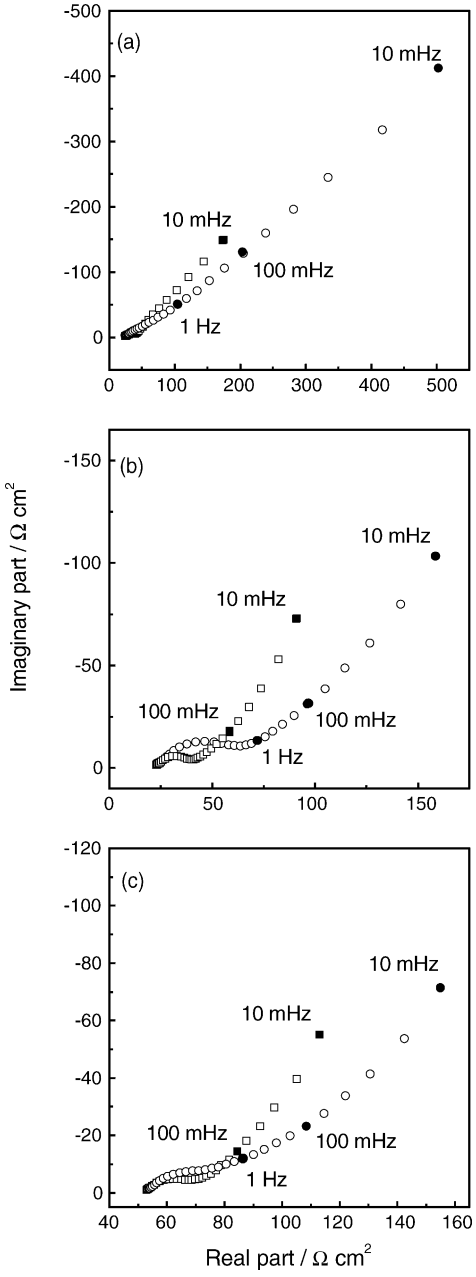

Fig. 7. Nyquist diagrams of different sample of nanotubes: (a) VO_x/hexadecylamine, (b) Na_yVO_x and (c) VO_x/$Pani_y$. Electrolytic solution 1.0 mol L^{-1} $LiClO_4$ in propylene carbonate. Mass of the electrode: 1.5 mg, (□) E_{dc} = 2.3 V and (◯) E_{dc} = 2.8 V.

the direction c) inside the nanotubes. Finally, an appropriate explanation for the conductivity of Na_yVO_x-NT would be the substitution of template molecules by Na^+ ions, which will diminish the distance between the oxide layers (33 Å for hexadecylamine and 10.55 Å for Na^+) allowing the tunneling of electrons through oxide layers.

As mentioned earlier, Nyquist diagrams show a semicircle and a region at low frequencies characterized by a straight line with a phase angle of 45°. Starting from the equation bellow

[28]:

$$|Z| = \left| \left(\frac{V_M}{\sqrt{2} z F D^{1/2} S} \right) \left(\frac{dE}{dx} \right) \omega^{-1/2} \right|$$

and using the slope of the impedance modulus $|Z|$ as a function of the inverse of square root of angular frequency ($\omega^{-1/2}$), the apparent coefficient diffusion was determined for the three electrodes. The value of dE/dx (≈6.5 V) was obtained in previous GITT experiments performed in our group [9], while the concentration of Li (x) was calculated by cyclic voltammetry with scan rate of 250 μV s^{-1} and mass = 1.5 mg for all electrodes, molar volume $V_M = 54\ cm^3\ mol^{-1}$ [9] and the geometric area of the electrode, $S = 2\ cm^2$. Fig. 8 shows the linear variation of the modulus of impedance versus the inverse of the square root of angular frequency ($\omega^{-1/2}$). The values of diffusion coefficients were calculated from the slope, and Fig. 9 shows the plot of the logarithm of apparent diffusion coefficient as a function of x_{Li} for the three samples. The high D_{Li} values found for the nanotubes, confirm the advantages of the utilization of a nanotubular material as intercalation electrode, especially for the case of VO_x/Pani$_y$-NT for which the diffusion coefficients are almost two orders of magnitude higher than nanotubes with template at low content of intercalated lithium. We can conclude that two important effects are responsible for these values: one is the nanotubular morphology which produces a diminution of the diffusion path of Li^+ ions and second, the diffusion rate could be higher because the electrostatic interactions between the Li^+ ion and the oxygen atoms of vanadium oxide are reduced due to the shielding effect proportioned by Pani and Na^+ ions. Finally, it is also observed a decrease of D_{Li+} with the increase of Li^+ content intercalated in the material. This is probably due to the electrostatic repulsion Li^+–Li^+ when the amount of lithium is high; even that this diminution is smaller than in V_2O_5 films as it was shown by Holland et al. [29]. Also, it can be note a decrease in D values when the content of Li increases in all nanotubes: this fact can be explained through unfavorable Li^+–Li^+ interactions when the content is approximately $x = 1$.

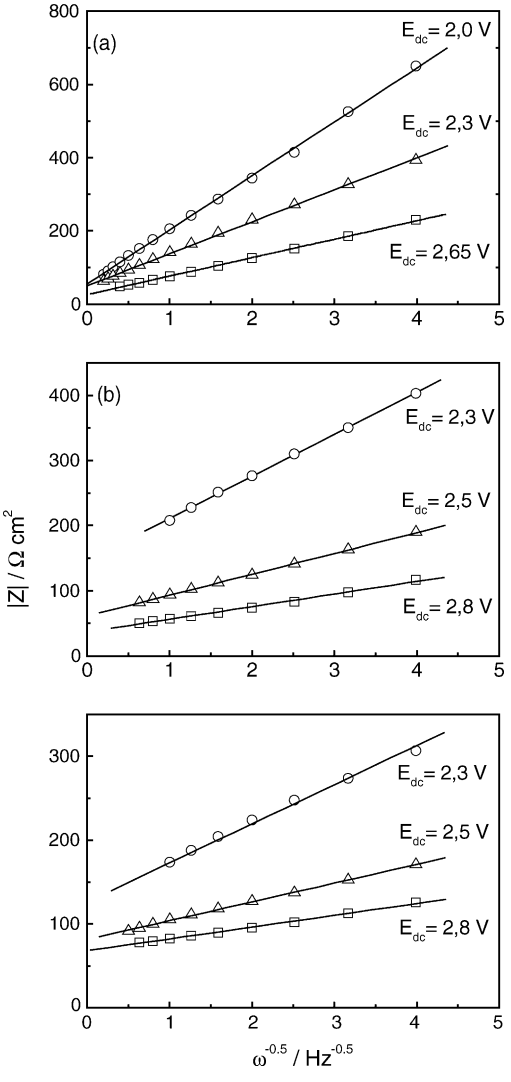

Fig. 8. Impedance modulus $|Z|$ as a function of the square root of angular frequency ($\omega^{-1/2}$) for (a) VO_x/hexadecylamine-NT, (b) Na$_y$$VO_x$-NT and (c) VO_x/PAni-NT at different applied potentials.

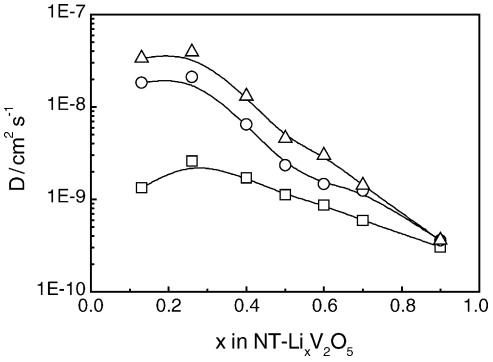

Fig. 9. Apparent diffusion coefficient in function of the intercalation degree of Li^+ for (□)VO_x/hexadecylamine-NT, (◯) Na$_y$$VO_x$-NT and (△)$VO_x$/Pani$_y$-NT.

Finally we would like emphasize the excellent properties of nanocomposites with tubular shape as intercalation materials. A comparison of the diffusion coefficient of nan-

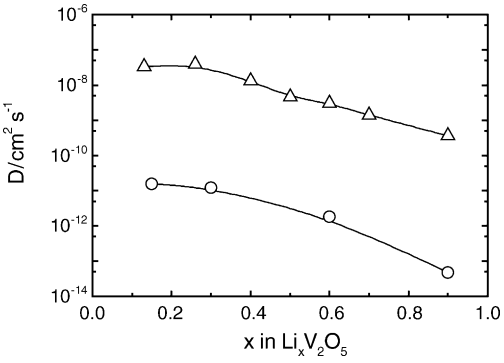

Fig. 10. Apparent diffusion coefficient in function of the intercalation degree of Li^+ for (△) VO_x/Pani$_y$-NT, and (◯) V_2O_5/Pani$_{0.3}$ xerogel (data taken from Ref. [19]).

otubes with amorphous xerogel V_2O_5/Pani nanocomposite (Fig. 10), showed that the performance of tubular composite present higher diffusion coefficient for all amount of lithium intercalated studied in this work, despite both are of the same chemical composition. The data here presented clearly indicate the relevant role played by the defined morphology at the nanoscale level.

4. Conclusions

This contribution demonstrates that it is possible to obtain a hybrid material with defined morphology for being used as electroactive material for lithium intercalation electrodes. The experimental tools used allowed a characterization of the local structure and morphology showing that the change of the surfactant by Pani does not modify the shape of the vanadium oxide nanotubes. These new hybrid nanostructures improve the diffusion kinetics of lithium intercalation due to their well-defined morphology, as it was shown by using electrochemical impedance spectroscopy. A comparison with hybrid nanocomposite without defined morphology has shown the potential application of nanotubular materials as high performing systems from the kinetics point of view.

Acknowledgments

We thank São Paulo State Foundation (FAPESP 02/08721-4), Electron Microscopy Laboratory (LME) at the Brazilian Synchrotron Light Laboratory (LNLS), Campinas, Brazil and the Laboratório de Espectroscopia Molecular (IQ-USP, Brazil) for financial support, HRTEM and Raman facilities, respectively. M. Malta thanks FAPESP for fellowship granted (00/00145-9).

References

[1] R. Tenne, Chem. Eur. J. 8 (2002) 5297–5304.
[2] S. Iijima, Nature 354 (1991) 56–58.
[3] C. Ye, G. Meng, Z. Jiang, Y. Wang, G. Wang, L. Zhang, J. Am. Chem. Soc. 124 (2002) 15180–15181.
[4] A. Rothschild, R. Popovtiz-Biro, O. Lourie, R. Tenne, J. Phys. Chem. B 104 (2000) 8976–8981.
[5] M.E. Spahr, P. Bitterli, R. Nesper, M. Müller, F. Krumeich, H.U. Nissen, Angew. Chem. Int. 37 (1998) 1263–1265.
[6] P. Gomez-Romero, Adv. Mater. 13 (2001) 163–174.
[7] C.-G. Wu, D.C. DeGroot, H.O. Marcy, J.L. Schindler, C.R. Kannewurf, Y.J. Liu, W. Hirpo, M.G. Kanatzidis, Chem. Mater. 8 (1996) 1992–2004.
[8] M. Lira-Cantu, P. Gomez-Romero, J. Electrochem. Soc. 146 (1999) 2029–2033.
[9] F. Huguenin, R.M. Torresi, D.A. Buttry, J.E. Pereira da Silva, S.I. Cordoba de Torresi, Electrochim. Acta 46 (2001) 3555–3562.
[10] F. Huguenin, R.M. Torresi, D.A. Buttry, J. Electrochem. Soc. 149 (2002) A546-A553.
[11] J.M. Reinoso, H.-J. Muhr, F. Krumeich, F. Bieri, R. Nesper, Helv. Chim. Acta 83 (2000) 1724–1733.
[12] M. Niederberger, H.-J. Muhr, F. Krumeich, F. Bieri, D. Günther, R. Nesper, Chem. Mater. 12 (2000) 1995–2000.
[13] F. Krumeich, H.-J. Muhr, M. Niederberger, F. Bieri, B. Schnyder, R. Nesper, J. Am. Chem. Soc. 121 (1999) 8324–8331.
[14] A. Dobley, K. Ngala, S. Yang, P.Y. Zavalij, M.S. Whinttingham, Chem. Mater. 13 (2001) 4382–4386.
[15] G.T. Chandrappa, N. Steunou, S. Cassaignon, C. Bauvais, P.K. Biswas, J. Livage, J. Sol–gel Sci. Technol. 26 (2003) 593–596.
[16] X. Chen, S. Xiaoming, Y. Li, Inorg. Chem. 41 (2002) 4524–4530.
[17] M.E. Spahr, P. Stoschitzki-Bitterli, R. Nesper, O. Haas, P. Novák, J. Electrochem. Soc. 146 (1999) 2780–2783.
[18] S. Nordlinder, K. Edström, T. Gustafsson, Electrochem. Solid-State Lett. 4 (2001) A129–A131.
[19] S. Nordlinder, J. Lindgren, T. Gustafsson, K. Edström, J. Electrochem. Soc. 150 (2003) E280–E284.
[20] B. Azambre, M.J. Hudson, Mater. Lett. 57 (2003) 3005–3009.
[21] Y. Cao, P. Smith, A. Heeger, Synth. Met. 48 (1992) 91–97.
[22] A.G. MacDiarmid, A.J. Epstein, Synth. Met. 65 (1994) 103–116.
[23] M. Wörle, F. Krumeich, F. Bieri, H.-J. Muhr, R. Nesper, Anorg. Allg. Chem. 628 (2002) 2778–2784.
[24] V.V. Fomichev, P.I. Vkrainskaya, T.M. Ilyin, Spectrochim. Acta Part A 53 (1997) 1833–1837.
[25] J. Harreld, H.P. Wong, B.C. Dave, B. Dunn, L.F. Nazar, J. Non-Crystal. Solid 225 (1998) 319–324.
[26] J.E. Pereira da Silva, D.L.A. de Faria, S.I. Córdoba de Torresi, M.L.A. Temperini, Macromolecules 33 (2000) 3077–3083.
[27] D. Rodrigue, J. Riga, J.J. Verbist, J. Chim. Phys. 89 (1992) 12091214.
[28] C. Ho, I.D. Raistrick, R.A. Huggins, J. Electrochem. Soc. 127 (1980) 343–350.
[29] G.P. Holland, F. Huguenin, R.M. Torresi, D.A. Buttry, J. Electrochem. Soc. 150 (2003) A721–A725.